# Mechanical Properties and Crystallization Behavior of Toughened Polyamide-6/Carbon Nanotube Composites

**J. M. Augustine, S. N. Maiti, A. K. Gupta**

*Centre for Polymer Science and Engineering, Indian Institute of Technology Delhi, New Delhi 110 016, India*

Received 25 March 2010; accepted 16 December 2010
DOI 10.1002/app.33975
Published online 31 January 2012 in Wiley Online Library (wileyonlinelibrary.com).

**ABSTRACT:** This article presents a study on nanocomposite prepared by incorporation of single wall carbon nanotube (SWNT) into the blend of polyamide-6 (PA-6) and ethylene–propylene–diene elastomer grafted with maleic anhydride (EPDM-*g*-MA), with varying SWNT content from 1 to 3% with the fixed composition of the matrix (PA-6: EPDM-*g*-MA being 65 : 35). Tensile properties of the rubber toughened PA-6 (i.e., PA-6/EPDM-*g*-MA blend) increased on incorporation of the nanofiller SWNT. Crystallization behavior studied through the analysis of the DSC crystallization exotherm showed distinct changes with varying content of the nanofiller. The SWNT nanofiller showed initially an enhancement of nucleation rate, which was overlapped with slowing down of crystallization growth rate, which results in smaller crystallinity and decreased crystal size. This slowing down of crystalline growth with increasing SWNT content is attributed to the presence of SWNT in the form of network like dispersion as seen by the scanning electron microscopic measurement. The decrease of crystallinity with increasing SWNT content is also shown by X-ray diffraction (XRD) measurements. The changes in XRD pattern indicate a variation in the relative proportion of $\alpha$ and $\gamma$ crystalline forms of PA-6 due to the presence of SWNT nanofiller.  J Appl Polym Sci 125: E478–E485, 2012

**Key words:** crystallization; single wall carbon nanotubes; polyamide-6; differential scanning calorimetry; X-ray diffraction

## INTRODUCTION

Use of nanoparticles in development of polymeric nanocomposites has become a leading research area owing to great potential of this new class of composites and ever increasing scope of their applications. Crystallization behavior of the polymer matrix in presence of nanofillers is important as it governs the morphology and properties of nanocomposites. Among the various nanofillers used for such composites, nanoclays and carbon nanotubes have been widely studied for development of nanocomposites with various polymers.[1–3] Two types of carbon nanotubes, multiwall carbon nanotubes (MWNT) and single wall carbon nanotubes (SWNT), have been used for development of polymer nanocomposites.[4] In this article, we present a study of the effect of SWNT on mechanical properties and crystallization of the crystallizing component (i.e., polyamide-6) of the matrix comprising of a blend of polyamide-6 (PA-6) with an elastomer ethylene–propylene–diene elastomer grafted with maleic anhydride (EPDM-*g*-MA) for compatibilization, at a fixed composition (65 : 35). This polymer blend constituting the matrix is called toughened PA-6 for brevity. Incorporation of elastomer improves impact properties with accompanying loss of tensile strength and stiffness. The nanofiller is used to compensate for this loss of tensile properties, without adversely affecting the impact properties of the rubber toughened PA-6.

The nanocomposites were prepared by melt mixing and the effect of varying composition of SWNT were studied on tensile and impact properties, crystallization behavior, and dispersion morphology.

## EXPERIMENTAL

### Materials

The PA-6 M28RC grade, was produced by Gujarat State Fertilizers and Chemicals, Vadodara, India having MFI 28g/cm$^3$ [230°C and 2.16 Kg load]. EPDM-*g*-MA, having 0.1–0.4% of MA grafting having density 0.88 g/cm$^3$ was produced by Pluss Polymers, Gurgaon, India. The single wall carbon nanotubes (SWNT soot) were purchased from Carbon Solutions (Riverside, CA), having diameter 2–10 nm with a bundle length of approximately 1–5 μm and density $\sim$ 1.2–1.5 g/cm$^3$. Morphology of SWNT soot is given by transmission electron microscopic and scanning electron microscopic (SEM) picture (Figs. 1 and 2).

*Correspondence to:* A. K. Gupta (akgncute@hotmail.com).
Contract grant sponsor: Department of Science and Technology, Govt. of India, New Delhi, India

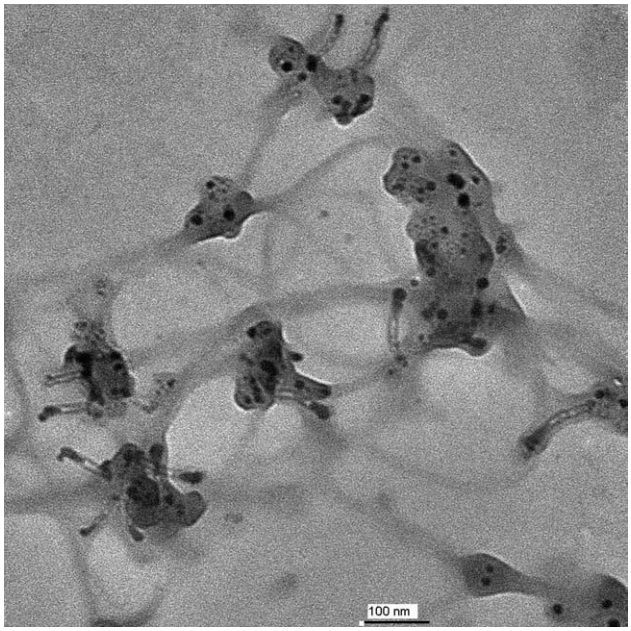


**Figure 1** Transmission electron micrograph of SWNT soot dispersed in acetone.

### Processing

The nanocomposites of the rubber toughened PA-6 were produced by melt mixing in two steps: first, melt compounding of the EPDM-*g*-MA and PA-6 and second, melt compounding of the toughened PA-6 with SWNT. The mixing was done in a counter rotating twin screw extruder at rpm 25 with temperature profile 220-235-250-240°C. The SWNT and the rubber toughened PA-6 pellets were premixed in a tumbler and fed to the twin screw extruder. The extruded strands were water cooled and granulated, and subsequently injection molded to make test specimens on a Demag L and T PFY 40 injection molding machine using temperature profile of 220–250°C. Sample nomenclature and composition is given in Table I. Before processing, the materials were properly dried in a vacuum oven (PA-6: 80°C for 4 h, EPDM-*g*-MA: 60°C for 3 h, PA-6/EPDM-*g*-MA: 80°C for 6 h).

### Mechanical properties

Tensile tests were performed at ambient temperature according to ASTM D 638 standard on a Zwick Universal Tester, model Z010 (Zwick USA LP, Kennesaw, GA) at a cross-head speed of 50 mm/min using a gauge length of 60 mm. The stress was calculated on the basis of cross-sectional area of the underformed samples. Modulus, tensile strength, and elongation at break were measured. The Izod impact strength of notched specimens was determined on a pendulum hammer type Ceast Impactometer (ASTM D256). The notch depth was 2.5 mm and notch angle was 45°. Five specimens which were dried in air oven at 60°C for 12 h and tested for each composition and averages of the data are reported. All the measurements were carried out at ambient temperature.

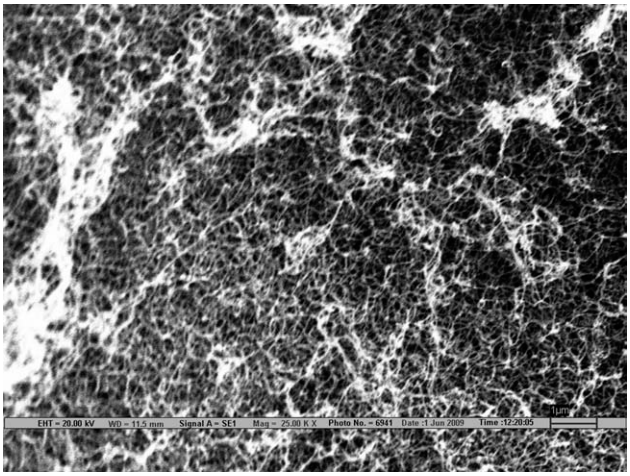

**Figure 2** SEM image of SWNT soot.

### Morphology

SEM of the fracture surfaces of the nanocomposite samples after liquid nitrogen fracture was done on Carl Zeiss EVO 50.

### Differential scanning calorimetry

Differential scanning calorimetric (DSC) measurements were done on Perkin–Elmer Pyris7 with temperature calibrated with indium to record the crystallization exotherms and the melting endotherms of the composites. The first heating scan from 30°C to240°C at10°C/min was recorded then the samples were maintained at 240°C for 1 min to delete any thermal history. The samples were then cooled at 10°C/min from 240 to 30°C under nitrogen atmosphere to record the crystallization exotherm.

### Thermogravimetry

Thermal degradation was measured by thermogravimetric analysis on a Perkin–Elmer Pyris7 thermal

**TABLE I**
**Composition and Nomenclature of the Samples**

| Sample code | PA6 (wt %) | EPDM-*g*-MA (wt %) | SWNT (wt %) |
|---|---|---|---|
| PA6 | 100 | 0 | 0 |
| Toughened PA6 (TN1) | 65.00 | 35 | 0 |
| TN2 | 65.13 | 34.83 | 0.05 |
| TN3 | 64.35 | 34.65 | 1.0 |
| TN4 | 63.70 | 34.30 | 2.0 |
| TN5 | 63.05 | 33.95 | 3.0 |

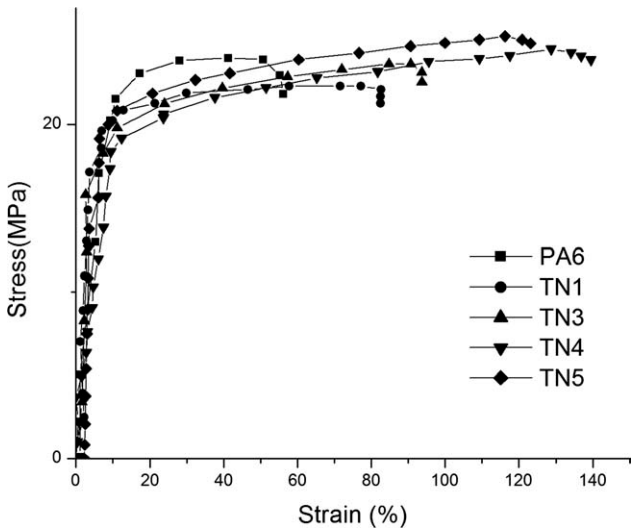


**Figure 3** Tensile stress–strain curves of toughened PA6 and its composites with SWNT at varying contents of the nanofiller at ambient temperature.

analysis system in a dynamic atmosphere of nitrogen from 50 to 750°C at a heating rate of 20°C/min.

### X-ray diffraction

The wide angle X-ray diffraction (WAXD) patterns were recorded on an X-ray powder diffractometer using CuKα radiation on the instrument (PANalytical Co. X'pert PRO, Netherlands).

## RESULTS AND DISCUSSION

### Mechanical properties

Figure 3 shows the representative stress–strain curves of the different compositions of the nanocomposites and the results are summarized in Table II. The tensile strength and modulus of PA-6 decreased on incorporation of the elastomer. This is an expected behavior of rubber toughened polymer system. Addition of the nanofiller SWNT from 1 to 3% produced slight increase of tensile strength. Modulus on the other hand increases significantly (about 25% increase over the entire range of SWNT content) with increasing SWNT content. Elongation at break which increased substantially on incorporation of the ethylene–propylene–diene (EPDM) elastomer to PA-6 shows further increase on addition of the SWNT nanofiller. In other systems reported earlier,[3] elongation at break is decreased by the incorporation of filler.

This observed improvement of tensile strength and modulus produced by the addition of SWNT is not encouraging in comparison with the composites of PA-6 with other less-expensive nanofillers such as MWNT[5]. Better dispersion and functionalization of SWNT is required to achieve desired property improvements. Other possibility for such poor improvement of tensile properties could be the effect of elastomer phase in these composites which may cause discontinuity of stress transfer and agglomeration of SWNTs and intertube slippage within bundles.

**TABLE II**
**Mechanical Properties of PA6/EPDM-*g*-MA/SWNT Composites**

| Sample | Tensile strength (MPa) | Tensile modulus (MPa) | Elongation to break (%) |
|---|---|---|---|
| PA6 | 72.8 | 424.6 | 56.4 |
| TN1 | 22.8 | 206.9 | 86.4 |
| TN3 | 24.4 | 214.8 | 92.4 |
| TN4 | 24.5 | 237 | 117.7 |
| TN5 | 24.9 | 245.7 | 109.2 |

### Izod impact strength

Table III shows Izod impact strength values for PA-6 and the nanocomposites. The pure PA-6 shows a notched impact strength 127 J/m. Addition of rubber to PA-6 causes a large increase in the Izod impact strength value as reported earlier.[6] On incorporation of rubber, the value of impact strength increases to 1044 J/m. Addition of the nanofiller SWNT produces slight decrease of the impact strength from 1044 to 780 J/m in the studied range of SWNT content, which is six times higher than the value for the pristine PA-6. Thus, we can say that the nanofiller SWNT has imparted an increase in stiffness to the rubber toughened PA-6 retaining the impact strength to a sufficiently high value. On the contrary, Zhang et al.[6] reported that incorporation of another nanofiller organoclay initially decreases the impact strength and further addition improves it.

### Crystallization behavior

Figure 4(a) shows crystallization exotherm recorded during cooling cycle and Figure 4(b) shows melting endotherms recorded subsequently during heating cycle for the toughened PA-6/SWNT composite

**TABLE III**
**Izod Impact Strength of PA6/EPDM-*g*-MA/SWNT Nanocomposites**

| Sample | Impact strength(J/m) |
|---|---|
| PA6 | 127.6 |
| TN1 | 1044 |
| TN2 | 1008 |
| TN3 | 932 |
| TN4 | 920 |
| TN5 | 780 |

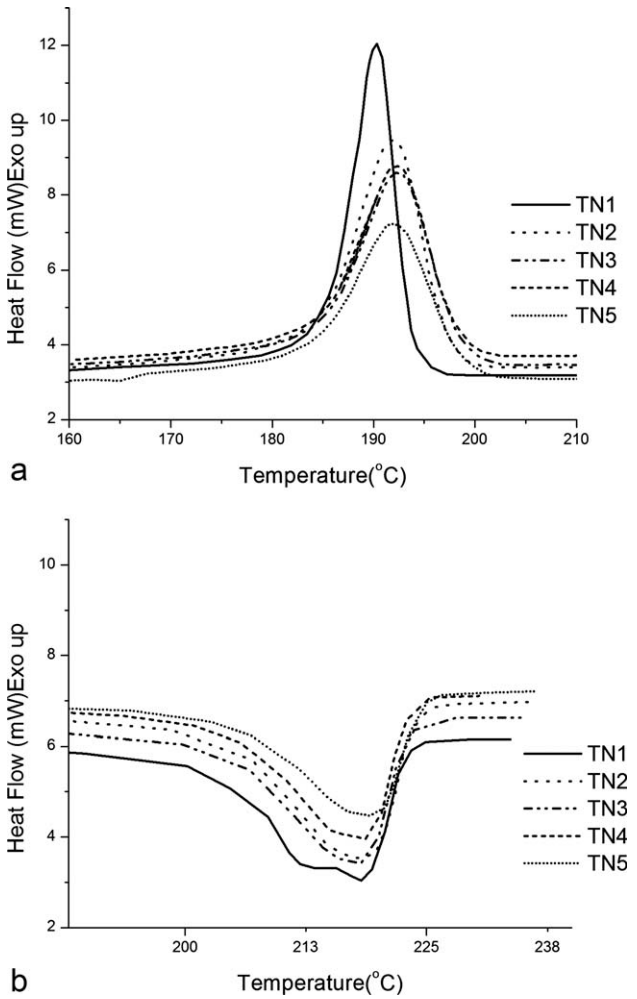


**Figure 4** DSC cooling (a) and heating (b) curves for toughened PA6 and the SWNT composites.

containing varying amount of the nanofiller (SWNT).Changes in the characteristic parameters of the crystallization exotherm are shown in Table IV. The characteristic parameters of the exotherm are peak temperature ($T_p$), onset temperature ($T_{onset}$) corresponding to the starting point of the exotherm, initial slope of the exotherm ($S_i$), crystallization enthalpy ($\Delta H$) determined from the area of the exotherm which is proportional to degree of crystallinity of the crystallizing component (i.e., PA-6), and the peak width at half height ($\Delta W$) which is indicative of crystal size distribution. Significance of these parameters and their relation with crystallization behavior and the resulting morphology are discussed elsewhere.[7] It is observed that $T_{onset}$ and $T_p$ increase on initial addition of SWNT at 0.5% content, and thereafter the trend of increase slows down at SWNT content 1% and above.

This increase in the onset and peak temperatures may be interpreted as an increase of the rate of the process, by time–temperature equivalence principle. The $T_{onset}$ increases more rapidly than $T_p$ indicating greater effect on the initial process (i.e., onset of crystallization or "nucleation'') than the process related to $T_p$ (i.e., the combined process of "nucleation'' and "growth'' occurring between $T_{onset}$ and $T_p$).

This observed difference in the variation of $T_{onset}$ and $T_p$ with increasing content of the nanofiller SWNT reveals a role of the nanofiller on crystallization behavior such that the SWNT enhances nucleation but slows down growth rate. The slowing down of the growth rate may be attributed to restriction to molecular chain mobility caused by the presence of SWNT nanofiller. Unlike particulate nanofiller, the carbon nanotubes may form irregular net-like dispersion which may cause obstruction to molecular chain mobility of PA-6 resulting in slow growth step of crystallization. The effect of SWNT on "growth'' step superimposes on the effect on "nucleation'' step right from the beginning such that the initial slope becomes smaller than the $S_i$ for unfilled toughened PA-6. This slowed growth of crystallization in presence of SWNT is corroborated by the decrease of crystallinity with increasing content of SWNT, shown in Table IV through values of crystallization enthalpy $\Delta H_c$.

Thus, the effect of SWNT filler on crystallization of PA-6 may be described as SWNT having inherent tendency to enhance nucleation of PA-6, but it does not produce significant increase in crystallinity of PA-6 due to net-like dispersion of nanotubes or large

**TABLE IV**
**Differential Scanning Calorimetry Data for Toughened PA6/SWNT Nanocomposites Under Heating and Cooling Conditions**

| | | Crystallization parameters(cooling at 10°C) | | | | |
|---|---|---|---|---|---|---|
| Sample | $T_{onset}$ (°C) | $T_p$ (°C) | $\Delta H_C$ (J/g) | $\Delta W$ (cm) | $T_m$ (°C) | $S_i$[a] |
| TN1 | 193.7 | 190.3 | 49.6 | 0.5 | 220.8 | 28.6 |
| TN2 | 197.2 | 191.8 | 45.1 | 0.8 | 221.4 | 8.1 |
| TN3 | 198.6 | 192.5 | 42.7 | 0.85 | 221.0 | 5.6 |
| TN4 | 198.2 | 192.4 | 39.2 | 0.9 | 221.0 | 5.6 |
| TN5 | 198.8 | 192.0 | 41.2 | 1.0 | 221.5 | 4.0 |

[a] Slope of initial part of crystallization exotherm at the higher temperature side.

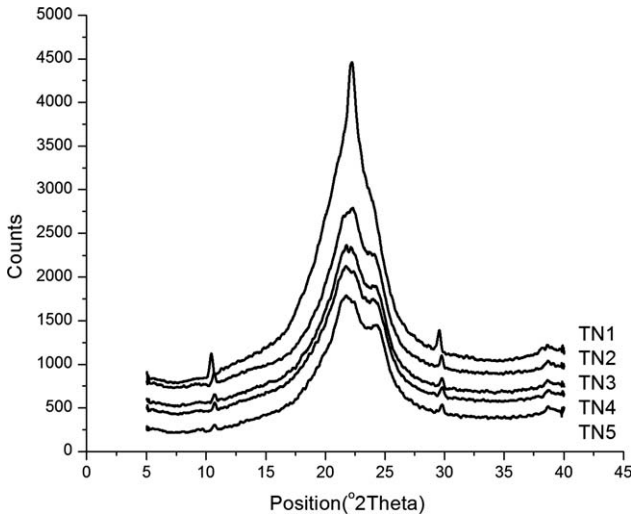


**Figure 5** XRD patterns of toughened PA6 and its nanocomposites.

agglomerates of SWNT obstructing chain mobility of PA-6. The nucleation-assisting role of SWNT has been also reported for PP/SWNT[8] and PA-6/SWNT[9] by other authors.

Initial slope ($S_i$) being lower for the case of higher $T_{onset}$ is unusual, unlike the results reported for PP/SWNT[8] system. Initial slope has combined effect of nucleation and growth process, hence the higher $T_{onset}$ accompanied by lower slope may be interpreted as SWNT acting as nucleating agent and the slowing down of growth may be attributed to nanotube network to obstruct chain mobility of PA-6 decreasing crystallization.

The mutually opposite trends of variation of $S_i$ and $\Delta W$, which is generally found as a condition of self consistency in this "five parameter" approach for analysis of crystallization exotherm[7] is obeyed by these data (Table IV) where the decrease of $S_i$ on addition of SWNT is accompanied by an increase of $\Delta W$. Higher value of $\Delta W$ (or the broader exotherm peak) implies wider distribution of crystallite size. Higher value of $S_i$ indicates faster rate of nucleation, corresponding to a situation somewhat similar to simultaneous creation of all nuclei, which on growth give rise to uniform size of the crystallites, i.e., the narrow distribution of crystal size or the narrow peak width $\Delta W$.

In case of the crystalline melting temperature ($T_m$) [Fig. 4(b) and Table IV], no significant change is observed on incorporation of SWNT, which may be due to not much change of the crystal size of PA-6. Similar results are reported for PA-6/SMA encapsulated SWNT composites.[9] Figure 4(b) shows doublet shape of melting peak for rubber toughened PA-6, showing the existence of either mixed crystal structure of PA-6 (i.e., α and γ form) or a combined process of melting and recrystallization during the heating cycle.

To supplement the DSC observations of crystallization of PA-6 in presence of the nanofiller SWNT, X-ray diffraction (XRD) studies were carried out. PA-6 crystallizes in α and γ form. Thermodynamically more stable form is α and the appearance of γ form is influenced by several factors such as polymer chain mobility (i.e., resistance to crystallization), cooling techniques, presence of moisture etc.[8] The WAXD patterns of toughened PA-6 and the composites are shown in Figure 5, and the parameters are given in Table V. In Figure 5, toughened PA-6 shows two peaks at $2\theta = 22.2^\circ$ and $24.1^\circ$ corresponding to α form[10,11] implying the absence of γ form. This supports one of the two possible reasons given above for the observed double peak shape of the melting endotherm, i.e., the double peak in the melting endotherm is due to recrystallization occurring during heating. The SWNT filled composites show one additional peak at $2\theta = 21.5^\circ$ corresponding to γ form.[8] Introduction of SWNT cause the decrease of chain mobility of PA-6 which favors the formation of γ crystals. This is reported earlier in PA-6/MMT clay nanocomposites.[8]

The crystallinity of toughened PA-6 and toughened PA-6/SWNT composites was calculated using the equation

$$X\% = \{I_c/(I_c + I_a)\} \times 100 \quad (1)$$

where $I_c$ is the intensity (height) of crystalline peak and $I_a$ is the intensity of amorphous peak. From data in Table V, it is seen that the crystallinity of toughened PA-6 decreased by the addition of nanofiller. Crystallite size can be calculated using Debye-Sherrer equation.[12]

$$L = k\lambda/\beta_0 \cos\theta \quad (2)$$

where $L$ is the crystallite dimension. θ is the incident angle, λ is wavelength of X-ray ($\lambda = 1.54$ Å), $\beta_0$ is the breadth of pure diffraction line, and $k$ is the shape factor of crystallite ($k$ is taken 0.89, as $\beta_0$ is defined as breadth at half-maximum intensity of the diffraction peak). Table V shows the values of the crystallite size for α peak. The crystallite size of α

**TABLE V**
**XRD Parameters of Toughened PA6/SWNT Composites**

| Sample | Crystallinity (%) | Crystallite size (L) (A°) (α) |
|---|---|---|
| TN1 | 37.26 | 135.5 |
| TN2 | 34.07 | 70.6 |
| TN3 | 32.37 | 76.2 |
| TN4 | 30.08 | 71.0 |
| TN5 | 31.9 | 69.5 |

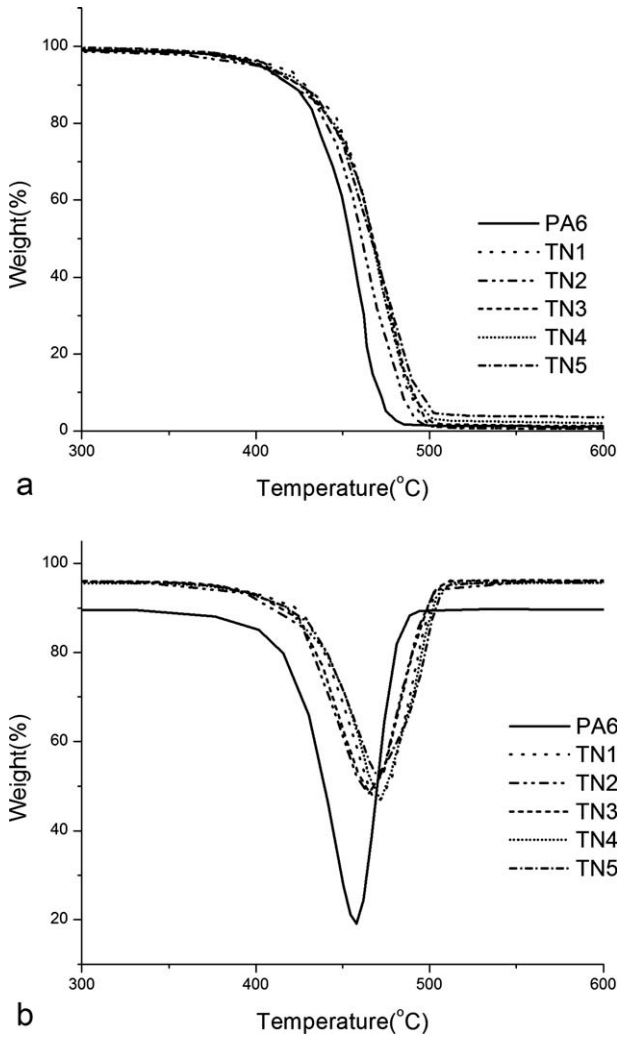


**Figure 6** TGA (a) and DTG (b) curves of the composites.

form of PA-6 shows a significant decrease on initial incorporation of the nanofiller with respect to the value for PA-6, followed by little variation with increasing SWNT content. This decrease of crystallite size is in accordance with the decrease in crystallinity.

### Thermogravimetric analysis

Thermal degradation temperature of toughened PA-6 and its composites containing varying amount of SWNT in nitrogen atmosphere was determined by thermogravimetric analysis (TGA). The TGA thermograms are shown in Figure 6. For toughened PA-6, the degradation starts at 443°C and gets completed at 488°C. Hence sample can be considered as stable up to 443°C in nitrogen atmosphere. The peak of DTG curves gives temperature corresponding to maximum degradation ($T_{max}$). In the DTG curve of toughened PA-6, the peak appeared at 470°C. The parameters obtained from TGA analysis is given in Table VI. Both $T_{onset}$ and $T_{max}$ of the blend increased with the incorporation of SWNT, indicating enhancement in thermal stability because of the incorporation of carbon nanotubes (CNTs). Similar increase of thermal stability were reported when MWNTs were incorporated in PA-6,10,PA10,10,PA-6, and in CNT/PA-6/GF.[5,10,13,14]

**TABLE VI**
**TGA Parameters of PA6 and Its Toughened Nanocomposites**

| Sample | $T_{onset}$ (°C) | $T_{max}$ (°C) |
|---|---|---|
| PA6 | 433 | 471 |
| TN1 | 443 | 488 |
| TN2 | 438 | 484 |
| TN3 | 445 | 490 |
| TN4 | 444 | 488 |
| TN5 | 441 | 491 |

Since thermal degradation of a polymer begins with chain cleavage and radical formation, the CNTs in the composites act as radical scavengers and hence improving the thermal stability of the polymers. Since CNTs exhibit a high intrinsic thermal conductivity of 200–3000 W/mK at room temperature,[15] its incorporation into polymers should lead to

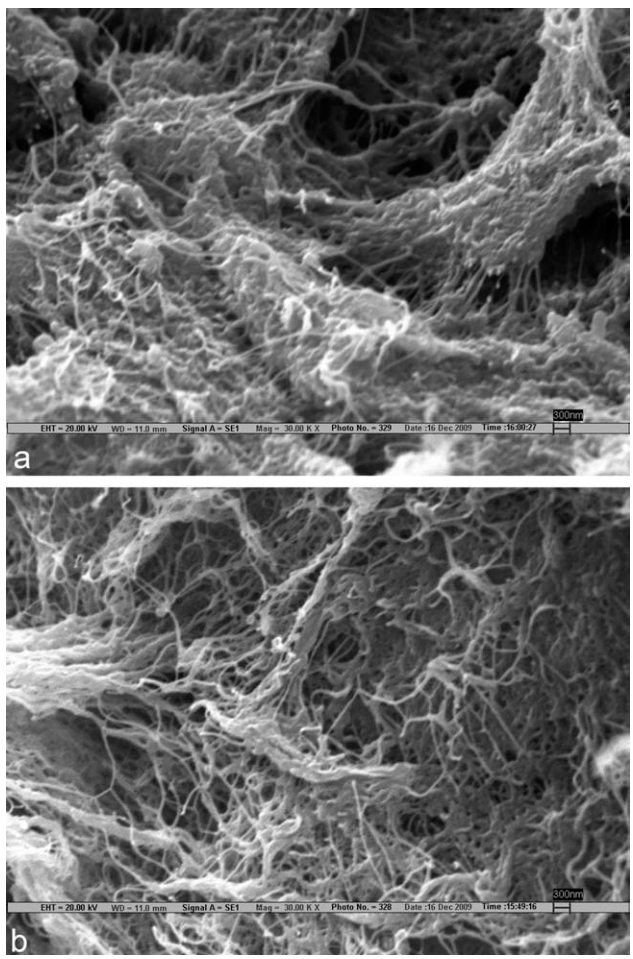


**Figure 7** SEM images of fractured surface of composite containing (a) 2% SWNT (b) 3% SWNT.

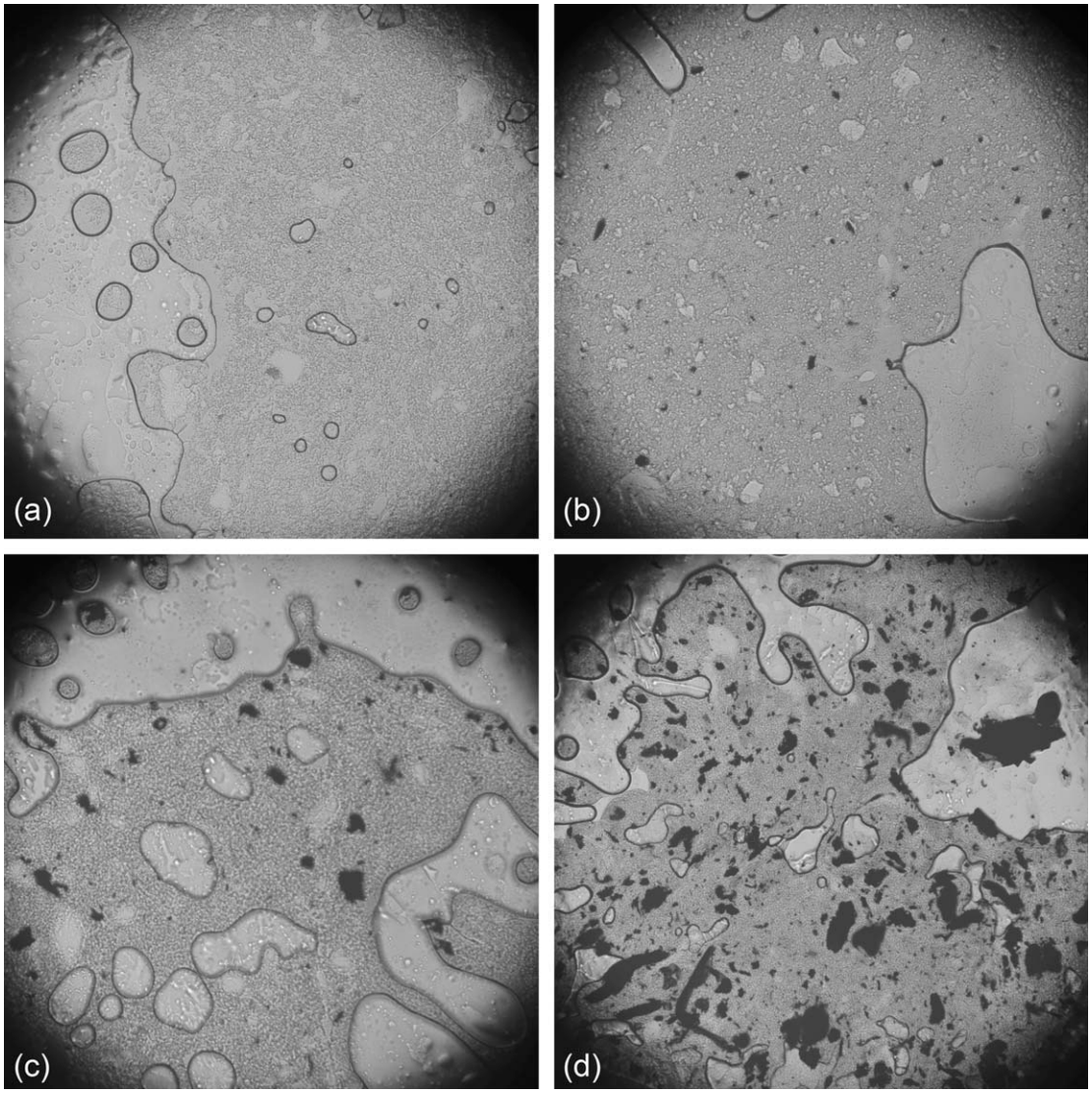


**Figure 8** Polarized optical micrographs of (a) toughened PA6 and toughened PA6/SWNT composite containing (b) 1%, (c) 2%, and (d) 3% SWNT at 245°C.

increases of the thermal conductivity resulting in better heat transport and enhanced thermal stability for the nanocomposite materials.[16]

### Morphology

The representative SEM photographs of the cross-sectional fracture of composites are shown in Figure 7. Cross-sections of the composites were prepared by fracturing the toughened polyamide-6 composites at liquid nitrogen temperature to produce fractured surface morphology. Typically, the carbon nanotubes in the fractured sample appear to be very long, wavy, and are lumped together. This type of morphology is an indication of highly agglomerated carbon nanotubes and weakly bonded with the matrix. The polarized optical microscope shows the agglomerated particles in the polymer–nanocomposite melt (Fig. 8).

The carbon nanotubes are apparently separated from the matrix without breaking the nanotubes, indicating their poor adhesion with the matrix. A similar kind of morphological observation was reported in epoxy/SWNT composites where a typical fracture surface consisted of a loose network of SWNT bundles, which had been pulled out of the matrix during deformation.[17]

## CONCLUSIONS

The composites show significantly higher toughness than PA-6. The property loss in rubber toughened polymers is common feature, *viz*. gain in impact strength is accompanied by loss of tensile stiffness and strength. Like other reinforcing fillers, carbon nanotubes (particularly the SWNT used in this work) produce reinforcement of PA-6/EPDM

elastomer blend at sufficiently low content, i.e., 1–3% without any significant loss in impact strength. The crystallization behavior of PA-6 is affected such that the inherent tendency of SWNT of enhancing nucleation rate is superimposed by the opposing effect of the nanotube network slowing down the growth rate. The net effect is of decreasing crystallinity and crystal size. The rubber toughened PA-6 showed better thermal stability than PA-6, while addition of nanofiller improved the thermal stability of the blends only marginally. XRD study exhibited a gradual transition from $\alpha$- to a mixture of $\alpha$ and $\gamma$-phase with increasing nanofiller content.

## References


1. Goa, J.; Zhao, B.; Itkis, M. E.; Bekyarova, E.; Hu, H.; Kranak, V.; Yu, A.; Haddon, R. C. J Am Chem Soc 2006, 128, 7492.
2. Goa, J.; Itkis, M. E.; Yu, A.; Bekyarova, E.; Zhao, B.; Haddon, R. C. J Am Chem Soc 2005, 127, 3847.
3. Saeed, K.; Park, S. Y. J Appl Polym Sci 2007, 106, 3729.
4. Iijima, S. Nature 1991, 56, 354.
5. Chen, G. X.; Kim, H. S.; Park, B. H.; Yoon, J. S. Polymer 2006, 47, 4760.
6. Zhang, L.; Wan, C.; Zhang, Y. Polym Eng Sci 2009, 49, 209.
7. Jafari, S. H.; Gupta, A. K. J Appl Polym Sci 1999, 71, 1153.
8. Fornes, T. D.; Paul, D. R. Polymer 2003, 44, 3945.
9. Bhattacharyya, A. R.; Pötschke, P.; Häubler, L.; Fischer, D. Macromol Chem Phys 2005, 206, 2084.
10. Pan, B.; Yue, Q.; Ren, J.; Wang, H.; Jian, L.; Zhang, J.; Yang, S. Polym Test 2006, 25, 384.
11. Valentini, L.; Biagiotti, J.; Kenny, J. M.; Santucci, S. J Appl Polym Sci 2003, 87, 708.
12. Kang, M.; Myung, S. J.; Jin, H. J. Polymer 2006, 47, 3961.
13. Zeng, H.; Gao, C.; Wang, Y.; Watts, P. C. P.; Kong, H.; Cui, X.; Yan, D. Polymer 2006, 47, 113.
14. Zhiqi, S.; Stuart, B.; Dong, Y. W.; Patrick, M.; Mel, D.; Januar, G. Compos Sci Technol 2009, 69, 239.
15. Yang, D. J.; Wang, S. G.; Zhang, Q.; Sellin, P. J.; Chen, G. Phys Lett A 2004, 329, 207.
16. Huxtable, S. T.; Cahill, D. G.; Shenogin, S.; Xue, L.; Ozisik, R.; Barone, P.; Usrey, M.; Stano, M.S.; Siddons, G.; Shim, M.; Keblinski, P. Nat Mater 2003, 2, 731.
17. Ajayan, P. M.; Schadler, L. S.; Giannaris, C.; Rubio, A. Adv Mater 2000, 12, 750.